DOI 10.24425/aee.2024.148860

Passivity-based control strategy for resonant converter based on Euler–Lagrange model

YAJING ZHANG[1], WEIHAO LIANG[1]✉, XIUTENG WANG[2], LIFEN LI[3]

[1]*School of Automation, Beijing Information Science & Technology University*
No. 12 Qinghe Xiaoying East Road, Haidian District, Beijing, China

[2]*Branch of Resource and Environment, China National Institute of Standardization*
No. 4 Zhi Chun Road, Haidian District, Beijing, China

[3]*School of Information Science and Technology, Yanching Institute of Technology*
No. 808 Yingbin Road, National High-tech Industrial Development Zone
Dongyanjiao, Beijing, Hebei, China

e-mail: zhangyajing@bistu.edu.cn, ✉ 1293091007@qq.com, wangxt@cnis.ac.cn, lilifen@yit.edu.cn

(Received: 29.05.2023, revised: 02.02.2024)

Abstract: The LLC resonant converter is a widely used DC/DC converter that offers the benefit of enabling soft switching compared to classical DC/DC converters. However, traditional PI control strategy based on a linear model has drawbacks such as slow dynamic response and poor anti-interference performance. To overcome the shortage, a passivity-based control strategy based on the Euler–Lagrange (EL) model is proposed in this paper to improve the dynamic performance of the half-bridge LLC resonant converter. In addition, the stability of the system based on the proposed strategy is analyzed and verified. Further, the effectiveness and performance of the proposed strategy is verified in the simulation by comparing with the traditional PI controller. Finally, a prototype was built to verify the dynamic performance of the LLC resonant converter based on the proposed control strategy.

Key words: LLC resonant converter, passivity-based control, PWM fixed frequency modulation, soft switching technology

1. Introduction

In recent years, the new energy industry has undergone rapid development, presenting higher challenges for power electronic conversion devices. As a result, researchers have conducted extensive research in pursuit of converters with high power, high efficiency, and high-power density. Meanwhile, the DC converters have drawn significant attention in recent years as an important link in power conversion [1–3]. In which, the LLC resonant converter has been widely used in various applications, such as data centers [4], server power supplies [5], microgrids [6], vehicle chargers [7]. The popularity of the LLC resonant converter can largely be attributed to its soft switching, low EMI, high efficiency, high power density, and electrical isolation. LLC resonant converters often requires a wide range of input or output voltages according to the practical applications, making them increasingly prevalent [8–10].

In the domain of LLC control strategies, traditional PI control has been associated with slow transient response speed and poor robustness. To overcome these challenges, researchers have proposed various nonlinear-based control strategies, such as sliding mode control, passivity-based control and adaptive control. Passivity-based control is an effective control approach that utilizes the energy characteristics of a system to design a controller, thereby enabling the system to maintain energy balance and avoid instability. This method exhibits robustness and can maintain system stability even with parameter disturbances and external disturbances. By performing mathematical derivations, it can derive control equations of the system and effectively design controllers. Additionally, passivity-based control can minimize energy loss, making the system more efficient in energy consumption. The implementation of the passivity-based control method is relatively straightforward and does not require complex controller architectures and algorithms. Furthermore, this method can be applied to a range of dynamic systems, including mechanical [11], electrical [12], and chemical systems. There are currently multiple nonlinear control methods applied to LLC resonant converters. For instance, the paper [13] proposed a robust control strategy that leverages second-order sliding mode technology for LLC resonant DC/DC converters, which improved the dynamic performance of the system. This method has good dynamic response, but its steady-state performance is not outstanding, with obvious output voltage ripple. Similarly, the paper [14] proposed a control strategy called super twisted sliding mode (STSMC) control, which is based on sliding film control. Notably, this control strategy does not require factorization of the internal parameters of the system. Instead, it only needs to solve the first-order derivative of the input, which is a computationally simple process. This method uses a reduced order model for modeling, which has a relatively simple calculation process and achieves good dynamic performance, but the output steady-state error is significant. A hybrid control strategy for LLC converters using linear active disturbance rejection control (ADRC) is proposed in the paper [15, 16]. In this article, frequency modulation is used to control the output voltage, while phase angle compensation is used to compensate for gain errors caused by changes in resonant components. Adopting this method improves the speed and anti-interference performance of the system without introducing additional switching losses. However, the use of this control strategy still has significant overshoot, and its advantage over PI control in terms of speed is limited. Furthermore, the paper [17] proposes a fuzzy adaptive PI controller for the voltage outer loop and a traditional PI controller for the current inner loop. Joint simulation of this approach using MATLAB and PLECS demonstrates the superiority of using a fuzzy adaptive PI controller, particularly with respect to voltage regulation.

However, the calculation method is relatively complex and needs to be improved in terms of parameter errors and magnetic integration. The paper [18] proposes a PWM strategy based on the event triggered control (ETC) method. This method can achieve fast and smooth startup of the system, and keep the resonant circuit current and capacitor voltage below the preset threshold. The biggest advantage of the ETC method is the smooth transition between the start-up and steady state. In [19, 20], a simplified optimal trajectory control (SOTC) for the LLC resonant converter is proposed. This article uses different control strategies and modulation methods in transient and steady-state situations. This method has good control effect, but the design is relatively complex. Compared with the above methods, passivity-based control variables are optional. The most convenient control method only requires sampling and controlling the output voltage of the system. It has the advantages of faster dynamic performance and no overshoot. When the system is in a stable state, there are no obvious ripple waves in the system.

In this paper, a novel passivity-based control strategy for LLC converters based on the Euler–Lagrange (EL) model is proposed, which exhibited superior performance of dynamic characteristics. The EL model of the LLC converter is built and the passivity of the system is verified. The EL model of the half-bridge LLC resonant converter is designed by injecting damping, enabling the system to reach steady state quickly, so as to obtain no overshoot, fast adjustment speed and good anti-disturbance characteristics. In the meanwhile, the feasibility and advantages of the passivity-based control strategy are verified with an LLC resonant converter based on MATLAB. Finally, a prototype was built to preliminarily verify the good dynamic performance of the LLC resonant converter under passivity-based control strategy when facing sudden load changes.

2. Working principle of a half-bridge LLC resonant converter

2.1. Circuit topology diagram of LLC resonant converter

The topology of a half-bridge LLC resonant converter is shown in Fig. 1(a), which is composed of four critical components. The first component is a switching circuit that comprises two main switches. The second component is a resonant tank that is composed of resonant inductance L_r, excitation inductance L_m, and resonant capacitor C_r. The third component is a full wave rectification circuit, which includes an ideal transformer and four diodes. Finally, the fourth component is a low-pass filter that consists of a filtering capacitor C_f and a load. The ideal output waveform for each part is presented in the figure to provide a comprehensive understanding of the system's functioning.

The equivalent circuit diagram of the half-bridge LLC resonant converter is shown in Fig. 1(b). This diagram provides an overview of the system's constituent elements and their voltage and current relationships, which lays the foundation for developing control strategies based on this topology.

The different variables depicted in Fig. 1(b) denote the DC input voltage as u_{in}, input voltage of the resonant circuit as u_{ab}, resonant inductance current as i_{Lr}, excitation inductance current as i_{Lm}, resonant capacitor voltage as u_{Cr}, output current of the resonant circuit as i_p, rectifier bridge output current as is, filter capacitor current as i_{cf}, converter output current as i_o, converter output voltage as uo, output resistance as R, and ratio of primary and secondary turns of the transformer as n. These variables are crucial to the operation of the half-bridge LLC resonant converter and are instrumental in developing effective control strategies for optimal system performance.

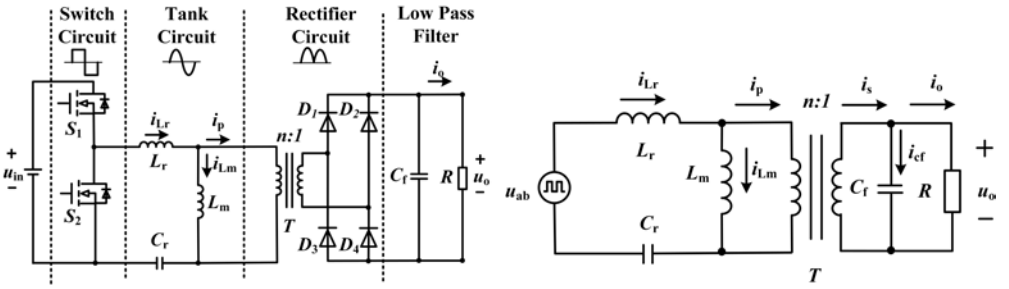

(a) Topology diagram of half bridge LLC resonant converter

(b) Equivalent circuit diagram of half bridge LLC resonant converter

Fig. 1. Half-bridge LLC circuit schematic of passivity-based controller based on EL model and its equivalent circuit diagram

3. Mathematical model of LLC resonant converter based on EL model

3.1. Design of passivity-based controller for LLC resonant converter

The dynamic equation of the equivalent circuit diagram of a half-bridge LLC resonant converter can be described as:

$$\begin{cases} L_r \dfrac{\mathrm{d}i_{Lr}}{\mathrm{d}t} + L_m \dfrac{\mathrm{d}i_{Lm}}{\mathrm{d}t} = u_{ab} - u_{Cr} \\ L_m \dfrac{\mathrm{d}i_{Lm}}{\mathrm{d}t} = \mathrm{sgn}\left(i_p\right) \cdot n u_o \\ C_r \dfrac{\mathrm{d}u_{Cr}}{\mathrm{d}t} = i_{Lr} \\ C_f \dfrac{\mathrm{d}u_o}{\mathrm{d}t} = n \cdot \mathrm{abs}\left(i_p\right) - \dfrac{1}{R} u_o \\ i_p = i_{Lr} - i_{Lm} \end{cases}, \tag{1}$$

where u_{ab}, sgn (i_p), and abs (i_p) are the nonlinear variables. The nonlinear variables present in Eq. (1) are as follows:

$$\mathrm{abs}\left(i_p\right) = \left|i_p\right|, \tag{2}$$

$$\mathrm{sgn}\left(i_p\right) = \begin{cases} 1 & i_p > 0 \\ -1 & i_p < 0 \end{cases}. \tag{3}$$

In the state equation, the dead time is not considered, and the upper and lower bridge arms can be regarded as conducting separately. Therefore, the switching signal $S = S_1 – S_2$ of the MOSFET transistor is introduced into the equation, where S_1 and S_2 are the driving signals of the upper and lower switch transistors, respectively. Taking the state variable $\boldsymbol{x} = [x_1, x_2, x_3, x_4]^T = [i_{Lr}, i_{Lm}, u_{Cr}, u_o]^T$,

the introduced state equation is as follows:

$$\begin{cases} L_r \dfrac{\mathrm{d}x_1}{\mathrm{d}t} + x_3 + nSx_4 = u_{ab} \\ L_m \dfrac{\mathrm{d}x_2}{\mathrm{d}t} - nSx_4 = 0 \\ C_r \dfrac{\mathrm{d}x_3}{\mathrm{d}t} - x_1 = 0 \\ C_f \dfrac{\mathrm{d}x_4}{\mathrm{d}t} - nS\left(x_1 - x_2\right) + \dfrac{1}{R}x_4 = 0 \end{cases}. \tag{4}$$

By expressing Eq. (4) in matrix form, an EL mathematical model of the LLC resonant converter can be obtained:

$$\boldsymbol{M}\dot{\boldsymbol{x}} + \boldsymbol{J}\boldsymbol{x} + \boldsymbol{R}\boldsymbol{x} = \boldsymbol{U}, \tag{5}$$

where:

$$\boldsymbol{M} = \begin{pmatrix} L_r & 0 & 0 & 0 \\ 0 & L_m & 0 & 0 \\ 0 & 0 & C_r & 0 \\ 0 & 0 & 0 & C_f \end{pmatrix}, \quad \boldsymbol{J} = \begin{pmatrix} 0 & 0 & 1 & nS \\ 0 & 0 & 0 & -nS \\ -1 & 0 & 0 & 0 \\ -nS & nS & 0 & 0 \end{pmatrix},$$

$$\boldsymbol{R} = \begin{pmatrix} 0 & 0 & 0 & 0 \\ 0 & 0 & 0 & 0 \\ 0 & 0 & 0 & 0 \\ 0 & 0 & 0 & \dfrac{1}{R} \end{pmatrix}, \quad \boldsymbol{U} = \begin{pmatrix} u_{ab} \\ 0 \\ 0 \\ 0 \end{pmatrix}$$

Because $\boldsymbol{J} = -\boldsymbol{J}^T$ is an antisymmetric matrix, it has the properties of the EL equation.

Set the desired balance point to:

$$\boldsymbol{x}^* = \left[x_1^* \, x_2^* \, x_3^* \, x_4^*\right]^T = \left[i_{Lr}^* \, i_{Lm}^* \, u_{Cr}^* \, u_o^*\right]^T. \tag{6}$$

The purpose of a passivity-based controller is to make the state variable $\boldsymbol{x}$ reach the steady state equilibrium point $\boldsymbol{x}^*$. Set the error of the state variable to $\boldsymbol{x_e} = \boldsymbol{x} - \boldsymbol{x}^*$, and the error energy storage function to:

$$H_e = \frac{1}{2}\boldsymbol{x_e^T}\boldsymbol{M}\boldsymbol{x_e}. \tag{7}$$

When $H_e \to 0, \boldsymbol{x_e} \to 0$, the purpose of control can be achieved.

The derivative of the error energy storage function for time is:

$$\dot{H}_e = \boldsymbol{x_e^T}\boldsymbol{M}\dot{\boldsymbol{x}}_{\boldsymbol{e}}. \tag{8}$$

To accelerate the convergence rate of H_e, a damped $\boldsymbol{R_a}$ is injected in the form of Formula (9).

$$\boldsymbol{M}\dot{\boldsymbol{x}}_{\boldsymbol{e}} + \boldsymbol{J}\boldsymbol{x_e} + \boldsymbol{R_d}\boldsymbol{x_e} = \boldsymbol{U} - \boldsymbol{M}\dot{\boldsymbol{x}}^* - \boldsymbol{J}\boldsymbol{x}^* - \boldsymbol{R}\boldsymbol{x}^* + \boldsymbol{R_a}\boldsymbol{x_e}. \tag{9}$$

In the formula, $\boldsymbol{R_d} = \boldsymbol{R} + \boldsymbol{R_a}$, where $\boldsymbol{R_d}$ is the positive definite matrix.

Substitute $\boldsymbol{M}\dot{\boldsymbol{x}}_{\boldsymbol{e}}$ into the derivative of the error energy function over time:

$$\dot{H}_e = \boldsymbol{x}_{\boldsymbol{e}}^{\boldsymbol{T}}[\boldsymbol{U} - \boldsymbol{M}\dot{\boldsymbol{x}}^* - \boldsymbol{J}(\boldsymbol{x}_{\boldsymbol{e}} + \boldsymbol{x}^*) - \boldsymbol{R}\boldsymbol{x}^* + \boldsymbol{R}_{\boldsymbol{a}}\boldsymbol{x}_{\boldsymbol{e}}] - \boldsymbol{x}_{\boldsymbol{e}}^{\boldsymbol{T}}\boldsymbol{R}_{\boldsymbol{d}}\boldsymbol{x}_{\boldsymbol{e}}. \tag{10}$$

To ensure $\dot{H}_e = -\boldsymbol{x}^{\boldsymbol{T}}\boldsymbol{R}_{\boldsymbol{d}}\boldsymbol{x}_{\boldsymbol{e}} < 0$, select a passivity-based controller:

$$\boldsymbol{U} = \boldsymbol{M}\dot{\boldsymbol{x}}^* + \boldsymbol{J}\boldsymbol{x} + \boldsymbol{R}\boldsymbol{x}^* - \boldsymbol{R}_{\boldsymbol{a}}\boldsymbol{x}_{\boldsymbol{e}}, \tag{11}$$

where:

$$\boldsymbol{R}_{\boldsymbol{a}} = \begin{pmatrix} R_a & 0 & 0 & 0 \\ 0 & R_a & 0 & 0 \\ 0 & 0 & \dfrac{1}{R_a} & 0 \\ 0 & 0 & 0 & \dfrac{1}{R_a} \end{pmatrix}, \quad \boldsymbol{x}_{\boldsymbol{e}} = \begin{pmatrix} i_{Lr} - i_{Lr}^* \\ i_{Lm} - i_{Lm}^* \\ u_{Cr} - u_{Cr}^* \\ u_o - u_o^* \end{pmatrix}.$$

Due to the fixed frequency modulation, the duty cycle d of switch S_1 needs to be introduced. The input-output relationship of the converter is as follows:

$$\frac{u_o}{u_{in}} = \frac{d}{0.5} \cdot \frac{M}{2n}. \tag{12}$$

In the formula M is the DC gain, taking the normal value $M = 1$, substituting Eq. (12) into the last equation of Eq. (4), taking d as the control variable, and i_{Lr}, i_{Lm}, u_{Cr}, u_o as the controlled variable, the control rates are as follows:

$$d = \frac{nR\left[nS(i_{Lr} - i_{Lm}) - C_f\dfrac{\mathrm{d}u_o^*}{\mathrm{d}t} - \dfrac{1}{R_a}(u_o - u_o^*)\right]}{Mu_{in}^*}. \tag{13}$$

Considering that i_{Lm} and i_{Cf} cannot be sampled in practical application, and the controller has better anti-load disturbance performance, equivalent substitution is needed. The input-output relationship between transformer and bridge rectifier is as follows:

$$nS(i_{Lr} - i_{Lm}) - C_f\frac{\mathrm{d}u_o^*}{\mathrm{d}t} = i_s - i_{cf} = i_o. \tag{14}$$

The optimal control rate can be obtained by substituting Formula (14) into Formula (13):

$$d = \frac{n\dfrac{u_o}{i_o}\left[i_o - \dfrac{1}{R_a}(u_o - u_o^*)\right]}{Mu_{in}^*}. \tag{15}$$

3.2. The system passivity proof of LLC resonant converter

Based on the mathematical model Formula (4) of the half-bridge LLC resonant converter, the following can be deduced:

$$\begin{cases} L_r i_{Lr} \dfrac{\mathrm{d}i_{Lr}}{\mathrm{d}t} = i_{Lr} u_{ab} - i_{Lr} u_{Cr} - i_{Lr} n S u_o \\ L_m i_{Lm} \dfrac{\mathrm{d}i_{Lm}}{\mathrm{d}t} = i_{Lm} n S u_o \\ C_r u_{Cr} \dfrac{\mathrm{d}u_{Cr}}{\mathrm{d}t} = u_{Cr} i_{Lr} \\ C_f u_o \dfrac{\mathrm{d}u_o}{\mathrm{d}t} = u_o n S (i_{Lr} - i_{Lm}) - \dfrac{1}{R} u_o^2 \end{cases} . \tag{16}$$

The equation of Eq. (16) is added to obtain the power equivalent equation of the system:

$$\frac{\mathrm{d}}{\mathrm{d}t} \left(\underbrace{\frac{1}{2} L_r i_{Lr}^2}_{H_{Lr}(t)} + \underbrace{\frac{1}{2} L_m i_{Lm}^2}_{H_{Lm}(t)} + \underbrace{\frac{1}{2} C_r u_{Cr}^2}_{H_{Cr}(t)} + \underbrace{\frac{1}{2} C_f u_o^2}_{H_{Cf}(t)} \right) = i_{Lr} u_{ab} - \frac{1}{R} u_o^2 . \tag{17}$$

In the formula: $H_{Lr}(t)$ and $H_{Lm}(t)$ are the electromagnetic energy stored in the resonance inductance and excitation inductance, respectively, and $H_{Cr}(t)$ and $H_{Cf}(t)$ are the electric field energy stored in the resonance capacitance and the filter capacitance, respectively.

The power equivalent equation of Eq. (17) is obtained by integrating 0 to t:

$$\underbrace{H(t)}_{\text{Energy at time } t} = \underbrace{H(0)}_{\text{Initial emergy}} + \underbrace{\int_0^t i_{Lr} u_{ab} \mathrm{d}\tau}_{\text{Supply energy}} - \underbrace{\int_0^t \frac{1}{R} u_o^2 \mathrm{d}\tau}_{\text{Dissipated energy}} . \tag{18}$$

In the formula: $H(t) = H_{Lr}(t) + H_{Lm}(t) + H_{Cr}(t) + H_{Cf}(t)$ is the total energy of the circuit, τ is an integral time constant. Since $u_o > 0$ and $R > 0$, a dissipative inequality can be obtained:

$$H(t) - H(0) < \int_0^t i_{Lr} u_{ab} \mathrm{d}\tau . \tag{19}$$

Equation (16) represents the input u_{ab}, output u_o, and energy supply rate $i_{Lr} u_{ab}$ of the system, proving that the system is strictly passive.

There is a close relationship between passivity and stability, and the positive definite storage function of a passive system can be used as a Lyapunov function. Passive systems are not a subset of stable systems, only passive systems with detectability conditions are stable.

Therefore, as long as the system is zero state observable or zero state detectable, the system is stable. There are definitions as follows: For a system, if $u(t) = 0$, $y(t) = 0$, shall be $\lim_{x \to \infty} x(t) = 0$. The system is defined as zero state detectable.

For the LLC resonant converter system, when the input and output of system is zero, as the time t tends towards infinity, the state variable $\boldsymbol{x}$ of the system can be concluded as zero. Therefore, the system is zero state detectable. Combined with the strict passivity of the system, the system is asymptotically stable.

Furthermore, a numerical simulation based on the Lyapunov exponent was conducted in MATLAB, in order to further verify the stability of the system [21]. Generally, the Lyapunov exponent represents the numerical characteristic of the average exponential divergence rate of adjacent trajectories in phase space. Also known as the Lyapunov feature index, it is one of the features used to identify several numerical values of chaotic motion. The formula of the Lyapunov exponent is as follows:

$$LEs = \lim \frac{1}{n} \sum_{k=0}^{n-1} \ln \left| \frac{\mathrm{d}f\,(x,d)}{\mathrm{d}x} \right|. \tag{20}$$

The Lyapunov exponent is often used to determine the chaos of a system, and images can intuitively determine whether a system or mapping is a chaotic system or mapping.

For the Lyapunov index LEs, different values have the following different meanings:

When $LEs > 0$, the system motion will enter a chaotic state, and the corresponding mapping is called chaotic mapping;

When $LEs < 0$, the motion state of the system tends to stabilize;

When $LEs = 0$, the system is in a stable state [22].

The numerical simulation algorithm of the LLC converter is to construct the Lyapunov function of the system through the Jacobian matrix of the system space state equation. In which the system state variable $\boldsymbol{x} = [x_1, x_2, x_3, x_4]^T = [i_{Lr}, i_{Lm}, u_{Cr}, u_o]^T$ and the duty cycle of the switch d are selected as the two Lyapunov variables.

The numerical simulation result of the system is shown in Fig. 2. In which, d represents the duty cycle of switch S_1. It can be seen that the value range of d is between 0 and 0.5, and the Lyapunov exponent is always less than zero. It can be seen that the system is asymptotically stable within this range.

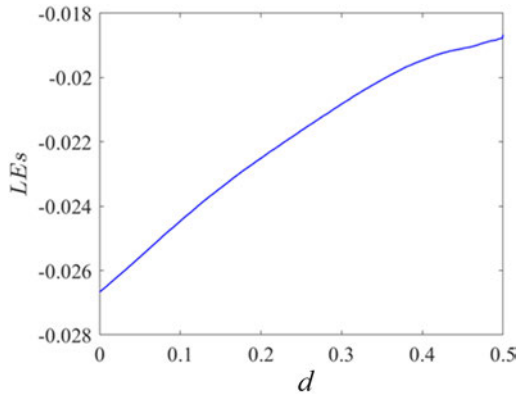

Fig. 2. Lyapunov exponent of the system

4. Simulation analysis of passivity-based controller for LLC resonant converter based on EL model

To verify the effectiveness of the control strategy proposed in this article, a simulation model of the LLC resonant converter with a rated power of 500 W was built in Simulink. PI control and passivity-based control were used as the control strategies for the circuit. The passivity-based control block diagram is shown in the Fig. 3.

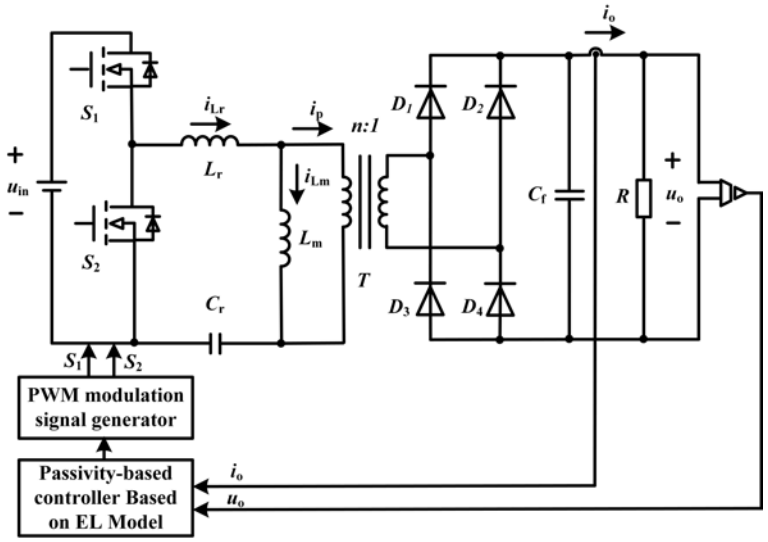

Fig. 3. Half-bridge LLC circuit schematic of passivity-based controller based on EL model

The output voltage and current of the circuit under different working conditions were compared to obtain simulation results of the steady-state and transient performance of the circuit. The PI control parameters are $k_p = 0.0025$, $k_i = 110$, and the passivity-based control injection damping R_a is 0.125 Ω. The circuit simulation parameters are shown in Table 1.

4.1. Steady-state performance of LLC based on proposed control strategy

The soft switching process during passivity-based control of the LLC resonant converter achieves zero voltage turn-on of the primary side and zero current turn-off of the secondary side, as shown in Fig. 4.

The comparison of steady-state performance simulation between passivity-based control and PI control is shown in Fig. 5. Among them, passivity-based control has no overshoot, steady-state error is 1.15%, and adjustment time is 8.67×10^{-5} s. The steady-state error of PI control can be ignored, with an overshoot of 15.6% and a rise time of 1.42×10^{-4} s, adjustment time is 8.39×10^{-4} s. From the perspective of adjusting time and overshoot, passivity-based control is superior to PI control.

Table 1. Circuit simulation parameters

Parameter name	Symbol	Value	Unit
Transformer ratio	n	3.96	
Switching frequency	f_s	160	kHz
Converter input voltage	u_{in}	380	V
Converter output voltage	u_o	48	V
Resonant inductance	L_r	21.7	μH
Magnetizing inductance	L_m	86.9	μH
Resonant capacitor	C_r	29.2	nF

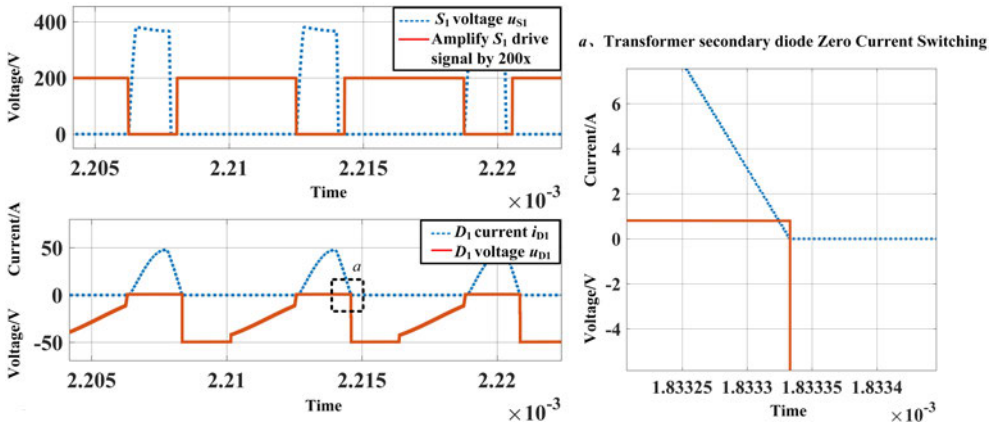

Fig. 4. LLC resonant converter soft switching process

4.2. Transient performance of LLC resonant converter based on the proposed control strategy

Figure 6 shows the waveform of the dynamic performance comparison between traditional PI control and passivity-based control when the expected output voltage suddenly increases. From the figure, it can be seen that the adjustment time under the traditional PI control strategy is $7.88.67 \times 10^{-5}$ s, and there is an overshoot of 1.1 v, while the adjustment time under the passivity-based control strategy is only 5.2×10^{-5} s. It can be seen that when the expected output voltage suddenly changes, the dynamic performance of the passivity-based control strategy is significantly better than that of PI control.

Figure 7 shows the waveform of the dynamic performance comparison between traditional PI control and passivity-based control when the input voltage suddenly increases. From the figure, it can be seen that under the traditional PI control strategy, there is a significant disturbance in the DC output voltage, and the stabilization speed is slow, while under the passivity-based control

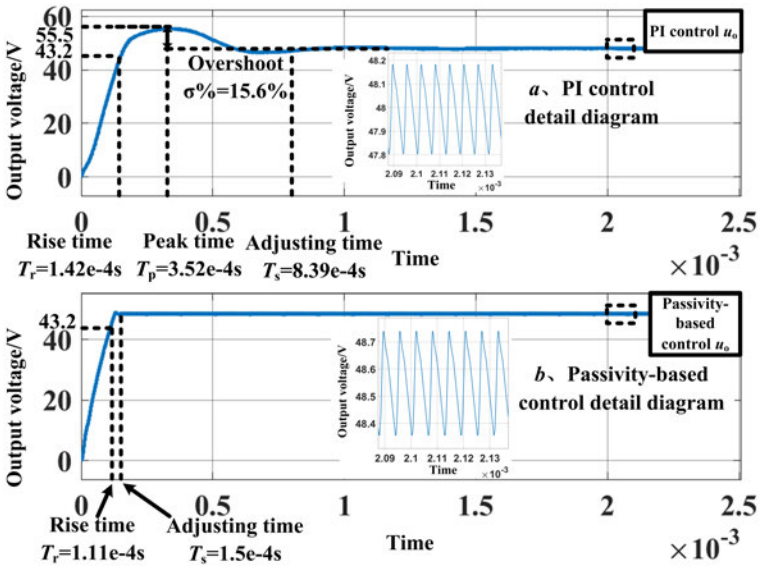

Fig. 5. Comparison of steady-state performance simulation of PI control and passivity-based control

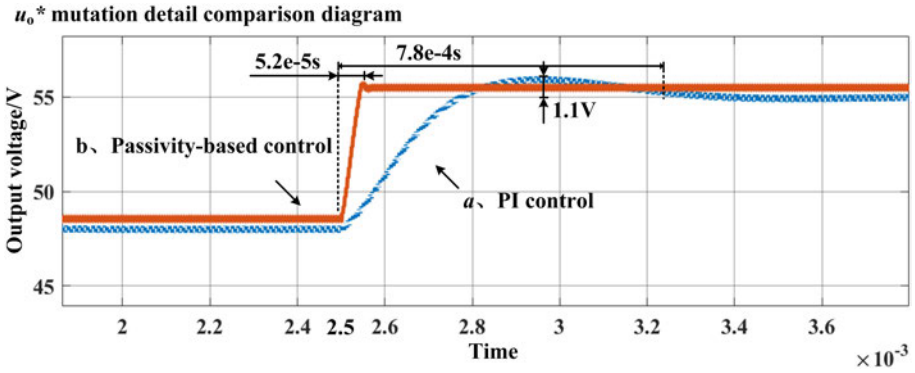

Fig. 6. Output voltage waveform when output voltage expectations spike

strategy, the DC output voltage quickly stabilizes without significant disturbance. By comparison, it can be seen that when the input voltage suddenly increases, the passivity-based control strategy improves the dynamic characteristics of the system.

Figure 8 shows the waveform of the dynamic performance comparison between traditional PI control and passivity-based control when the load suddenly changes. The combined resistance is 5 Ω, and the load suddenly changes by 50%. From the figure, it can be seen that when facing sudden changes in load and a sudden increase in output current, the adjustment time under passivity-based control is significantly faster than that under PI control, and there are significant disturbances in the output voltage and current under PI control. It can be seen that passivity-based control has good resistance to load disturbances compared to PI control.

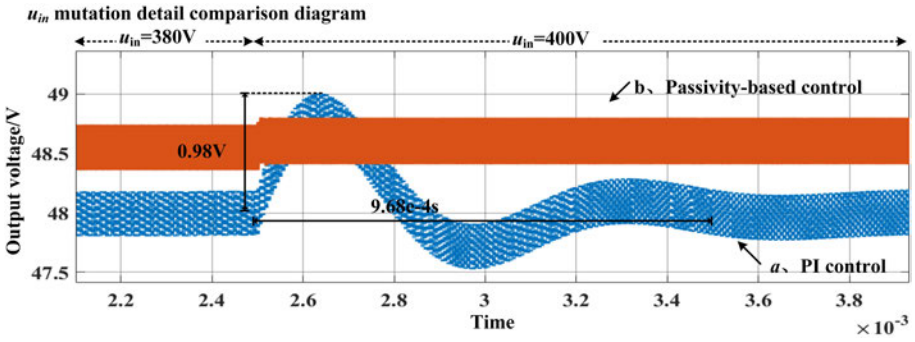

Fig. 7. Output voltage waveform when input voltage sudden rise

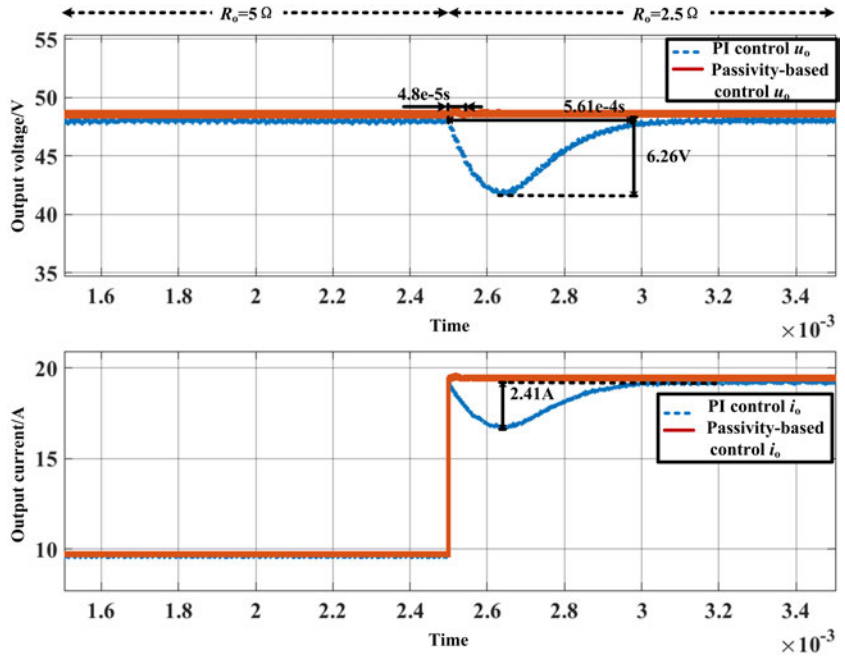

Fig. 8. Comparison chart of output current spikes due to sudden load changes

5. Experiment validation

In order to further verify the effectiveness of the passivity-based LLC resonant converter control strategy, a prototype of the LLC resonant converter was established. Figure 9 shows the important working waveforms of the LLC resonant converter, achieving a voltage reduction function from 200 V to 14 V.

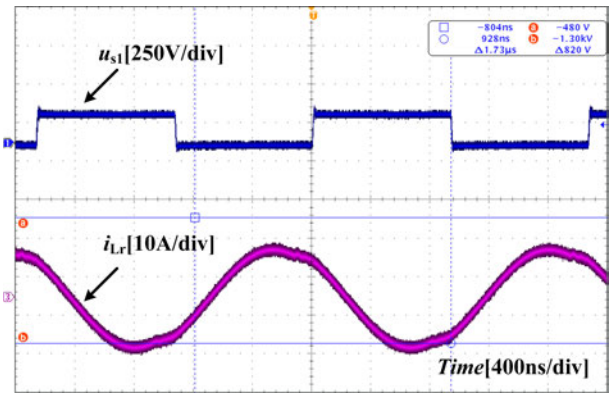

Fig. 9. LLC resonant converter switch S_1 voltage u_{S1} and resonant inductor current i_{Lr}

Figure 10 shows the waveform of the LLC resonant converter under passivity-based control when facing load disturbances. From the figure, it can be concluded that passivity-based control has good rapidity and does not produce severe fluctuations when facing load disturbances.

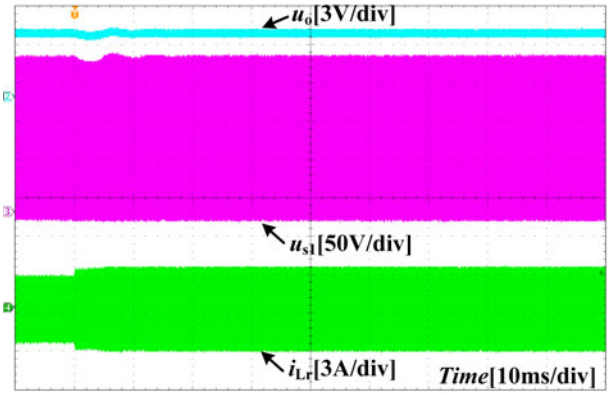

Fig. 10. Waveform diagram of load sudden change experiment under passivity-based control

6. Conclusions

In this paper, a passivity-based control strategy based on the EL model for the LLC resonant converter is proposed. Moreover, a passivity-based controller for a half-bridge LLC resonant converter was designed and verified by simulation and experiment. Furthermore, the stability of a system based on the proposed control strategy is analyzed and demonstrated. To further explore the feasibility and advantages of the proposed control strategy, a passivity-based controller for a half-bridge LLC resonant converter was developed using Simulink. The proposed control strategy

in both transient and steady-state situations has a better robust characteristic compared with the traditional PI controller. Finally, a prototype was built to preliminarily verify the good dynamic performance of the LLC resonant converter based on the proposed passivity-based control strategy.

Acknowledgements

Project Supported by National Natural Science Foundation of China (52237008, 52107176, 51777012) and Yanching Institute of Technology 2020 Major Science, Education and Research Projects (2020YITSRFZD203).

References

[1] Changzu A., Hongxia L., *Research on dual-mode switching of the new dual full-bridge topology of the beam supply*, Archives of Electrical Engineering, vol. 71, no. 4, pp. 1017–1034 (2022), DOI: 10.24425/aee.2022.142122.

[2] Jianfen Z., Chuangfang W., Dongwei X., *Design and analysis of the ferrite air-gapped cores for a resonant inductor*, Archives of Electrical Engineering, vol. 67, no. 3, pp. 579–589 (2018), DOI: 10.24425/123664.

[3] Leilei G., Mingzhe Z., Changzhou Y., Haizhen X., Yanyan L., *A model-free direct predictive grid-current control strategy for grid-connected converter with an inductance-capacitance-inductance filter*, Archives of Electrical Engineering, vol. 72, no. 1, pp. 23–42 (2023), DOI: 10.24425/aee.2023.143688.

[4] Junming Z., Guidong Z., Sanson S.Y., Bo Z., Yuan Z., *LLC resonant converter topologies and industrial applications – A review*, in Chinese Journal of Electrical Engineering, vol. 6, no. 3, pp. 73–84 (2020), DOI: 10.23919/CJEE.2020.000021.

[5] Yan-Kim T., Francisco D.F., Drazen D., *Open-loop power sharing characteristic of a three-port resonant LLC converter*, in CPSS Transactions on Power Electronics and Applications, vol. 4, no. 2, pp. 171–179 (2019), DOI: 10.24295/CPSSTPEA.2019.00017.

[6] Mohamed S., Vigna K.R., Awang J., Sanjeevikumar P., Mohamad P., Jiashen T., Dahaman I., *Three-Phase Series Resonant DC-DC Boost Converter with Double LLC Resonant Tanks and Variable Frequency Control*, in IEEE Access, vol. 8, pp. 22386–22399 (2020), DOI: 10.1109/ACCESS.2020.2969546.

[7] Huan L., Buxiang Z., Gao L., Tianlei Z., Shi C., Xiang Z., Jianping X., *Voltage-Mode Variable-Frequency Controlled LLC Resonant Power Factor Correction Converter and Its Accurate Numerical Calculation Analysis*, in IEEE Journal of Emerging and Selected Topics in Power Electronics, vol. 11, no. 2, pp. 1979–1994 (2023), DOI: 10.1109/JESTPE.2022.3230089.

[8] Ubaid A., Honnyong C., Nabeel N., Duc-Tuan D., *Integrated Current Balancing Transformer Based Input-Parallel Output-Parallel LLC Resonant Converter Modules*, in IEEE Transactions on Power Electronics, vol. 36, no. 5, pp. 5278–5289 (2021), DOI: 10.1109/TPEL.2020.3026929.

[9] Jakub K., Drazen D., *Equal Loss Distribution in Duty-Cycle Controlled H-Bridge LLC Resonant Converters*, in IEEE Transactions on Power Electronics, vol. 36, no. 5, pp. 4937–4941 (2021), DOI: 10.1109/TPEL.2020.3028879.

[10] Shuilin T., Frend C.L., Qiang L., *Equivalent Circuit Modeling of LLC Resonant Converter*, in IEEE Transactions on Power Electronics, vol. 35, no. 8, pp. 8833–8845 (2016), DOI: 10.1109/TPEL.2020.2967346.

[11] Youssif Mohamed Toum Elobait, Ahmed Hassan M. Hassan, *Tracking Control of Pneumatic Muscle Using Adaptive Passivity Based Control*, 2019 International Conference on Computer, Control, Electrical, and Electronics Engineering (ICCCEEE), Khartoum, Sudan, pp. 1–6 (2019), DOI: 10.1109/ICCCEEE46830.2019.9071057.

[12] Bingyuan W., Hui F., *The Buck-Boost converter adopting passivity-based adaptive control strategy and its application*, Proceedings of the 7th International Power Electronics and Motion Control Conference, Harbin, China, pp. 1877–1882(2012).

[13] Sijia G., Yue Z., Shuo S., Xingwei Wu., You Z., Jianxing Liu., *Sliding mode control of LLC resonant DC-DC converters*, 2016 IEEE 25th International Symposium on Industrial Electronics (ISIE), Santa Clara, U.S.A, pp. 1034–1037 (2016).

[14] Dexiang F., Chengzhong Z., Jinqiu S., Bin D., Wenlong D., Chenghui Z., *The super-twisting sliding mode control for half-bridge three-level LLC resonant converter*, 2022 6th CAA International Conference on Vehicular Control and Intelligence (CVCI), Nanjing, China, pp. 1–6 (2022).

[15] Chengzhong Z., Bin D., Jinqiu S., Qijun S., Chenghui Z., *A Modified Active Disturbance Rejection Control Strategy for Current Balance in Parallel LLC Resonant Converter*, 2022 34th Chinese Control and Decision Conference (CCDC), Hefei, China, pp. 3077–3082 (2022).

[16] Hao B., Dongjiang Y., Jinqiu S., Qijun S., Bin D., Chenghui Z., *Linear Active Disturbance Rejection Control of LLC Resonant Converters for EV Chargers*, 2020 Chinese Automation Congress (CAC), Shanghai, China, pp. 993–998 (2020).

[17] Tianpei C., Qihong C., Lei L., Liyan Z., Shuhai Q., *Research on full bridge LLC resonant converter based on fuzzy self-adaptive PI control*, 2017 32nd Youth Academic Annual Conference of Chinese Association of Automation (YAC), Hefei, China, pp. 132–137 (2017).

[18] Xuliang Y., Xiao H., Jingfang W., Guo X, Yuefeng L., Mei S., *A Soft Start-up Strategy of LLC Resonant Converter Based on Event Trigger Control*, 2020 IEEE 9th International Power Electronics and Motion Control Conference (IPEMC2020-ECCE Asia), Nanjing, China, pp. 1702–1705(2022).

[19] Weiyi F., Fred C.L., Paol M., *Simplified Optimal Trajectory Control (SOTC) for LLC Resonant Converters*, in IEEE Transactions on Power Electronics, vol. 28, no. 5, pp. 2415–2426 (2013), DOI: 10.1109/TPEL.2012.2212213.

[20] Chao F., Fred C.L., Qiang L., *Light load efficiency improvement for high frequency LLC converters with Simplified Optimal Trajectory Control (SOTC)*, 2015 IEEE Energy Conversion Congress and Exposition (ECCE), Montreal, QC, Canada, pp. 1653–1659 (2015).

[21] Czornik A., Nawrat A., Niezabitowski M., *On the stability of Lyapunov exponents of discrete linear systems*, 2013 European Control Conference (ECC), Zurich, Switzerland, pp. 2210–2213 (2013).

[22] Mojtaba A., Maryam D., Alireza K., Mohsen M., *Lyapunov Exponent based Stability Assessment of Power Systems*, 2019 6th International Conference on Control, Instrumentation and Automation (ICCIA), Sanandaj, Iran, pp. 1–5 (2019).